The following publication Kai Wang, Zhongqing Su, and Shenfang Yuan "A three-dimensional analytical model for interpreting contact acoustic nonlinearity generated by a "breathing" crack", Proc. SPIE 10170, Health Monitoring of Structural and Biological Systems 2017, 101701X (5 April 2017) is available at https://doi.org/10.1117/12.2258202.

A Three-dimensional analytical model for interpreting contact acoustic nonlinearity generated by a "breathing" crack

Kai Wang[a], Zhongqing Su*[a,b], Shenfang Yuan[c]
[a]Department of Mechanical Engineering, The Hong Kong Polytechnic University, Kowloon, Hong Kong SAR
[b]The Hong Kong Polytechnic University Shenzhen Research Institute, Shenzhen 518057, PR China
[c]State Key Lab of Mechanics and Control of Mechanical Structures, Nanjing University of Aeronautics and Astronautics, Nanjing 210016, P.R. China

ABSTRACT

Extending a two-dimensional analytical framework previously developed for understanding contact acoustic nonlinearity (CAN) in a beam-like structure bearing a contact crack[1], this study reports an analytical model for interpreting CAN induced due to the modulation from a "breathing" crack in a plate-like structure on propagating guided ultrasonic waves (GUWs) in a three-dimensional (3-D) scenario. The "breathing" crack is considered, in a 3-D manner, as a second source to excite additional wave fields. Thorough investigation of the interaction between the probing GUWs and the "breathing" crack leads to explicit, analytical and full-field description of additional wave fields. In this study, influences of reflected and diffracted waves by the crack on the motion of crack surfaces are scrutinized, yielding a depiction of the "breathing" behavior of the crack, beneficial for quantifying the crack-induced source at double frequency, with which the crack-induced nonlinearity (i.e. second harmonic) can be evaluated quantitatively, in conjunction with the use of an elasto-dynamic method. A nonlinearity index is consequently defined to represent the severity of the "breathing" crack. Results obtained from the 3-D model are compared with those from a finite element simulation, to affirm good agreement. This model does not request a benchmarking process against baseline signals for evaluation of damage.

Keywords: "breathing" crack; guided ultrasonic waves; analytical model; contact acoustic nonlinearity

1. INTRODUCTION

Fatigue cracks, inevitably existent in engineering structures subjected to cyclic loads during their service lifetime, are highly detrimental to engineering assets. Without timely awareness and remedial measures, the fatigue cracks in safety-critical components might lead to the catastrophic failure of the entire system and immeasurable loss[2]. Deployment of an effective non-destructive evaluation (NDE)[3] method can fulfill the desire for detection and identification of fatigue cracks before they reach a critical degree. However, the conventional NDE methods may suffer from limitations, including operation at a scheduled interval (with possibility to ignore fatigue cracks at initial stage), high cost, interruption to normal operation[4]. Most importantly, conventional NDE methods may perform the detection unsatisfactorily in terms of the sensitivity and reliability that they can offer. Aiming at developing a continuous and *in-situ* monitoring of fatigue cracks, structural health monitoring[5] (SHM) has been attracting increasingly intensive research efforts over decades.

Recent years have witnessed the wide application of guided ultrasonic waves (GUWs) in the development of SHM techniques for damage identification in metallic and composite structures[6-8]. Due to numerous applications of plate and shell-like structures in engineering practice, Lamb waves – the wave modality guided by a thin plate-like waveguide – are the most widely employed GUW modes. Lamb waves feature appealing properties including long-range propagation, entire thickness penetration, high sensitivity to structural damage. Conventional Lamb-wave-based SHM detects the damage by scrutinizing the changes in linear signal features at the frequency range in which the incident waves are exited, including delay of time-of-flight, wave reflection, transmission and mode conversion. Nevertheless, these

* Zhongqing.Su@polyu.edu.hk; phone: +852-2766-7818; fax: +852-2365-4703

methods are constrained to the detection of gross damage whose size is comparable with the wavelength of the selected Lamb wave mode[9-11].

In order to improve the sensitivity to damage of small scale, such as the fatigue cracks at incipient stage, the nonlinear features of GUWs induced by the fatigue cracks are exploited, to develop improved detection philosophy which could enhance the detectability towards undersized fatigue cracks. Amongst nonlinear features induced by various types of mechanism, the contact acoustic nonlinearity, originating from the "breathing" behavior of the contact fatigue cracks, holds tremendous potential to detect existence of fatigue cracks and further localize crack locations[12]. Under loading, the interface of a contact fatigue crack closes and opens periodically when probing waves traversing, leading to the clapping of crack surfaces and interval change of wave scattering at the crack. This "breathing" behavior introduces the time-dependent changes in scattered wave fields, leading to the generation of CAN. Representatively, by assuming a step-change of stiffness for material at the crack in one-dimensional scenario, Solodve *et al.*[13] revealed that only part of the probing waves can traverse a contact crack and the accordingly generated nonlinearity can be extracted from the rectified waves. Richardson[14] analytically studied the motion history of crack surfaces modulated by the traversing waves, yielding a similar prediction for the generation of CAN.

Although intense efforts have been directed to the fundamental investigation of CAN using numerical or experimental means, there are only few studies dedicated to the analytical interpretation of the generation of CAN and quantitative evaluation of fatigue cracks in two-dimensional (2-D) or even three-dimensional (3-D) scenarios which, however, are the case in reality. In 2-D and 3-D scenarios, the interaction between the probing waves and the "breathing" crack are highly complex, as a consequence of the existence of multiple GUW modes and mode conversion. The analytical depiction of wave propagation characteristics is therefore a daunting task. For guided waves in 2-D and 3-D scenarios, both finite propagating and infinite evanescent wave modes would be excited upon interaction between the incidence wave and the contact crack, and the converted wave modes (e.g. antisymmetric wave modes generated at the crack when symmetric waves traversing) would be induced as well. The difficulty imposed by these complexities greatly impedes the interpretation of CAN in 2-D and 3-D scenarios and the development of damage detection technique using CAN.

In the author's previous work[1], an analytical model has been proposed to develop an insight into the generation of CAN in 2-D scenario which gave an interpretation for the modulation mechanism of "breathing" crack on wave propagation and provided a quantitative prediction about the generated CAN. Extending the 2-D analytical framework previously developed, this paper aims at achieving an insight into the generation CAN and establishing an effective approach to identify and evaluate the fatigue crack in a 3-D scenario. In the present study, the "breathing" crack is considered as a second source, when probing waves traversing, to excite additional wave fields. An explicit, analytical and full-field depiction of the crack-induced wave source is obtained via a thorough investigation of the interaction between the probing GUWs and the "breathing" crack. Based on the depiction, CAN (i.e. second harmonic generation) can be quantitatively predicted in conjunction with the use of an elasto-dynamic method. A nonlinearity index is accordingly defined to represent the severity of the "breathing" crack, which is observed to have a monotonous relation with the crack parameters. With this prediction, the generation of CAN can be interpreted analytically and the crack is to be evaluated quantitatively.

This paper is organized as follows: in section 2, the "breathing" behavior of a contact fatigue crack is scrutinized when the crack interacts with the traversing waves, whereby the crack-induced source is obtained and the generation of high-order harmonics can be ascertained from the spectra of obtained wave fields. With this explicit depiction, the amplitude of accordingly generated second harmonics is predicted analytically using an elasto-dynamic method in section 3, whereby a nonlinear index is defined to evaluate the crack severity. Validation of the proposed method is accomplished in section 4 by comparing the analytical results with those obtained using a finite element method. Concluding remarks and discussions about the proposed method are included in section 5.

2. CAN INDUCED BY "BREATHING" CRACK

Consider a three-dimensional plate bearing the through-thickness fatigue crack, when the crack closes during the compressive phase of Lamb waves, the plate is assumed to be intact and the waves traverse the crack without distortion; when the crack opens during tensional phase of the traversing waves, as shown in Figure 1, the wave propagation is

modulated and thereby wave scattering is induced at the crack. As detailed in the author's previous work[1], the wave field during crack opening can be expanded as the superposition of incident waves and additional crack-related waves, and a crack-induced second source (CISS) spotted at the crack accounts for the generation of additional wave field. It is this CISS induced by the interaction of the open crack with Lamb waves that generates the reflection, transmission, diffraction and even mode conversion. The CISS is present when the crack opens and absent otherwise, and it is such a time-dependent feature of the CISS that leads to the generation of CAN manifested in the propagating waves, as typified by the second harmonics.

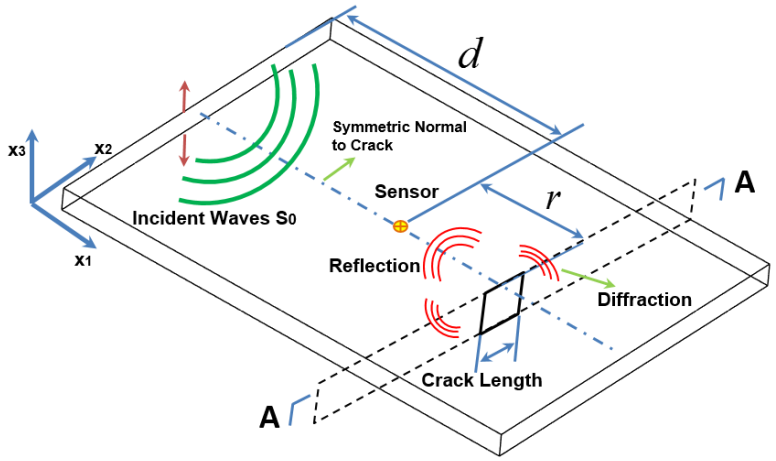

Figure 1 Schematic of a 3-D plate bearing a "breathing" crack and subjected to a point excitation

As analyzed in the author's previous work[1], scrutiny of the "breathing" behavior in the time domain composes the first step in interpreting the generation of CAN. Following the same way of analysis, the time for the closing and opening of the crack when probing waves traversing is first determined by canvassing the respective influence of each type of wave modes generated at the crack on the motion of crack surfaces. Considering the configuration of the crack and the mode shape of each type of wave mode, a beam of Lamb waves (fundamental symmetric wave mode S_0) is excited into the plate, since most of the energy is concentrated within the in-plane motion and thus it is more effective to trigger the "breathing" behavior. To circumvent the complexity imposed by the influence of the incident angel between the probing waves and the crack on the "breathing" behaviour, a beam of the selected Lamb waves (S_0) is uniformly excited to propagate perpendicularly to the crack. The sensor which records the in-plane displacement on top surface of the plate is located on the perpendicular bisector of the crack, as shown in Figure 1. Same as that in a 2-D scenario[1], the crack opens at the moment, denoted by t_{open} when the traversing waves turn from the compressional phase into the tensional phase. Upon crack opening, the interaction of traversing waves with the open crack induces reflection on the reflecting crack surface and diffraction around crack tips. It is worth noting that in the diffracted wave fields, accompanying the scattering of S_0 wave mode, there is a mode conversion occurring at the crack tip, introducing SH wave mode radiated out from the crack tips, as shown in Figure 2.

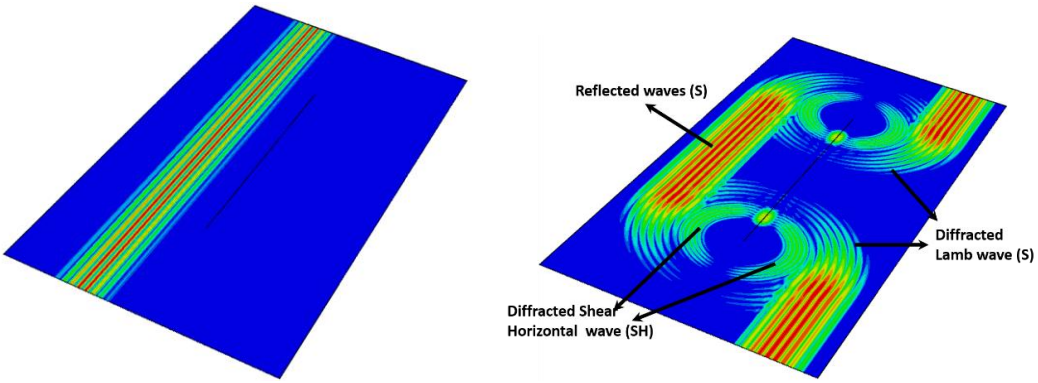

Figure 2 Snapshots of wave propagation in the plate bearing a "breathing" crack: (a) a beam of incident Lamb waves; (b) interaction of Lamb waves with the crack generating reflection, diffraction and mode conversion

The wave fields generated during the interaction of incident waves with an open crack can be decomposed into the superposition of the wave fields of incident waves, transmission/reflection and diffraction, as shown in Figure 2. The motion of points on crack surfaces can be depicted as:

$$\begin{aligned} u^{d+} &= u^{inc} + u^{ref} + u_{S0}^{dif} + u_{SH}^{dif}, \\ u^{d-} &= u_{S0}^{dif} + u_{SH}^{dif}. \end{aligned} \tag{1}$$

where u^{d+} and u^{d-} represent the displacement of points on the reflecting and transmitting surface of the crack, respectively. u^{inc} and u^{ref} denote the displacement induced by the incident waves and reflected waves, respectively. u_{S0}^{dif} and u_{SH}^{dif} represent the displacement induced by the diffracted S_0 wave and the diffracted SH wave, respectively.

The crack closes at the moment when the displacement of point on the reflecting surface equals that of point on the transmitting surface, yielding

$$u^{d+} = u^{d-} \ . \tag{2}$$

The reflecting crack surface is equivalent to a free end when the crack opens. An earlier study[15] has revealed that the displacement of point on the crack surface induced by the reflected waves equals that induced by the incident waves, *i.e.* $u^{ref} = u^{inc}$. Considering the crack configuration and normal incidence of probing waves, the displacement of crack surfaces induced by the diffracted S_0 wave mode (u_{S0}^{dif}) is trivial compared with that induced by other wave modes, and thus u_{S0}^{dif} can be neglected in what follows. Based on the above analysis, Eq. (2) can be re-written as

$$u^{inc} = u_{SH}^{dif} \ . \tag{3}$$

Solving Eq.(3) yields the time for crack closing, denoted by t_{close}. It has been proven[15] that when subjected to a concentrated force (corresponding to the crack tip in this case), the amplitude of the generated SH waves is of the same order as that of the S_0 mode. A qualitative estimation of the diffracted field is accordingly made since the analytical expression for the diffracted field is difficult and cumbersome to obtain which is not included in this study. Based on this estimation, the time for crack closing is approximated to be:

$$t_{\text{close}} = t_{open} + T_{inc} / 2 + t_{delay} / 2, \tag{4}$$

where T_{inc} is the period of incident waves and $t_{delay}/2$ is the time for the diffracted waves to propagate from the crack tip to the center of the crack.

As stated in the above, the "breathing" crack-induced source (CISS^{bre}) is present when the crack opens and absent otherwise, this case can be considered as the crack-induced source in an open crack case (CISS^{open}) being modulated by a window function $f(t)$ which has the following expression:

$$\begin{aligned} CISS^{bre} &= CISS^{open}\, e^{i\omega t} \times f(\mathrm{t}), \\ f(t) &= \begin{cases} 1, & t_{open} < t < t_{close} \\ 0, & t_{close} < t < t_{open} + T_{inc}. \end{cases} \end{aligned} \tag{5}$$

Figure 3 gives an illustration for the above-stated modeling process.

The spectrum of the crack-induced source CISS^{bre} can be obtained using the convolution between the incident wave period function $e^{i\omega t}$ and a window function $f(t)$. In the spectrum, the magnitude of each component can be ascertained. Therefore, the stress field induced by the "breathing" crack at double frequency can be obtained as

$$CISS^{bre}_{2f_0} = A_{2f_0} \times CISS^{open}\, e^{i2\omega t}. \tag{6}$$

3. PREDICTION OF AMPLITUDE OF SECOND HARMONICS

The second harmonics extracted from the reflected waves are ascertained to identify and evaluate the severity of the "breathing" crack. The reflected waves are generated by the CISS^{bre} on the reflecting surface which is explicitly obtained in section 2. It is worth noting that the CISS outside the crack surfaces is negligible compared with the CISS on the crack surfaces, and thus the CISS can be depicted as shown in Figure 4.

Considering that the scale of the crack in this study, measuring half of the wavelength of the incident Lamb waves at its maximum, can be ignored compared with the distance between the sensor and the crack, the CISS at the crack when it opens is equivalent to a point force whose amplitude can be calculated using the following integration over the crack surface.

$$CISS^{open} = \int_{Crack\ Surface} -\sigma^{inc} ds. \tag{7}$$

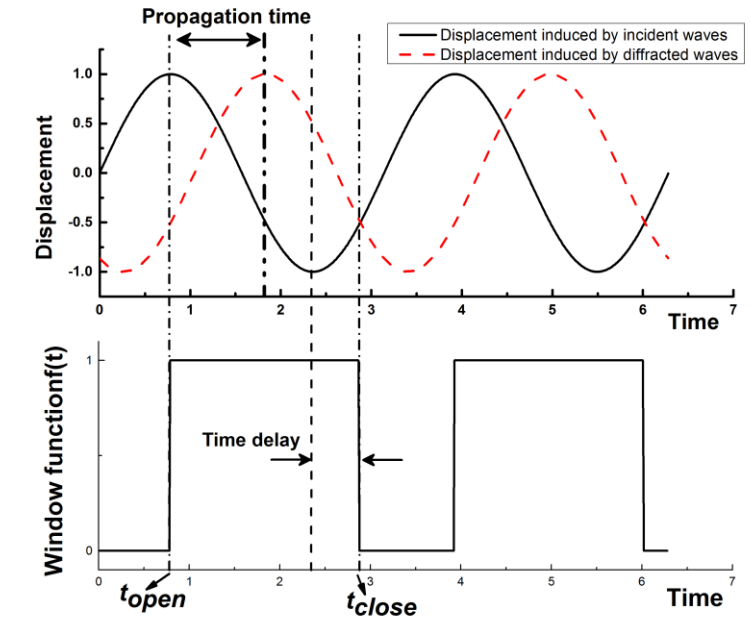

(a)

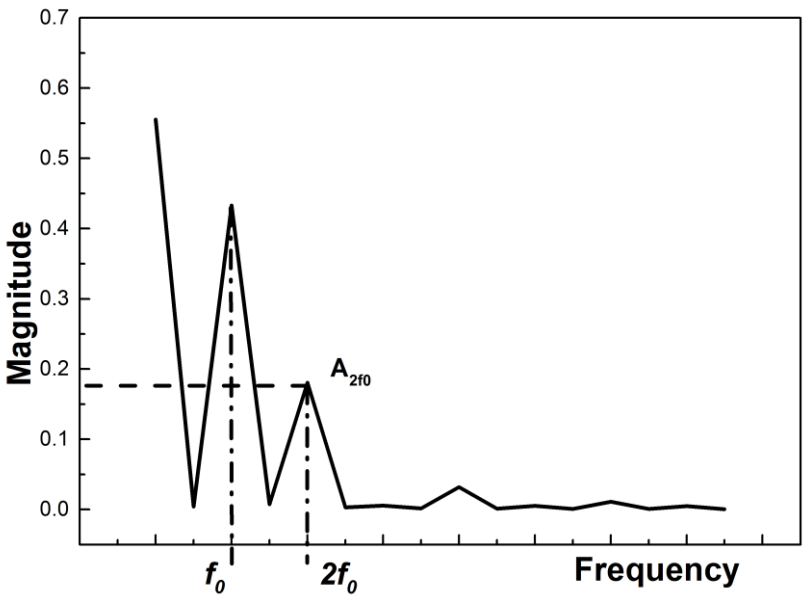

(b)

Figure 3 (a) Approximated modulation function; (b) spectrum of the CISS^{bre}

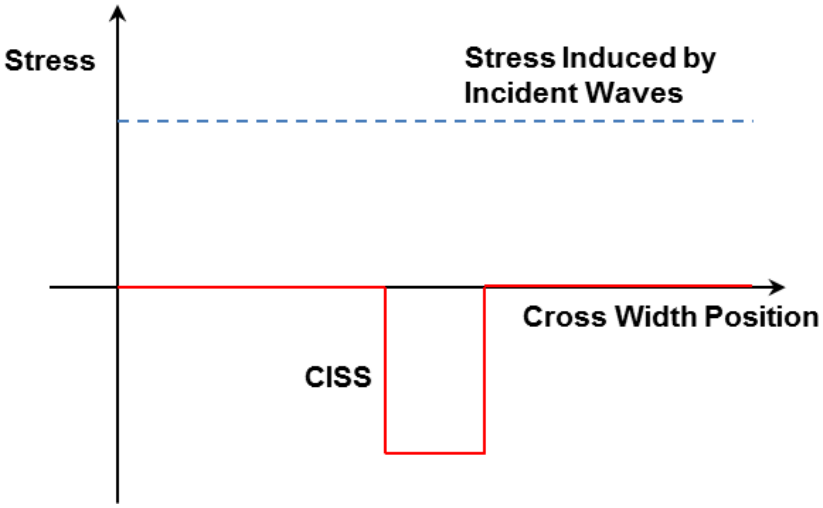

Figure 4 CISS in the plane A-A containing the crack

Given the explicit depiction of the $CISS_{2f_0}^{bre}$, the accordingly generated wave modes can be predicted using an elasto-dynamic method[16]. The detailed derivation procedures can be referred to elsewhere[15]. The displacement of second harmonics induced by the CISS can be predicted using

$$
\begin{aligned}
{}_{2f_0}u_{x_1}^{pr} &= A_{pr}^{S} U_S^{pr}(z)\left[H_0^2(k_{pr}r) - \frac{1}{k_{pr}r}H_1^2(k_{pr}r)\right], \\
A_{pr}^{S} &= \frac{k_{pr}}{4i}\frac{CISS_{2f_0}^{bre} U_S^{pr}(z)}{I_{prpr}^{S}}, \\
I_{mn} &= \int_{-h}^{h}\left[\sigma_{rr}^{Sm}(z)U_S^n(z) + \sigma_{rz}^{Sn}(z)W_S^m(z)\right]dz.
\end{aligned}
\tag{8}
$$

In the above, ${}_{2f_0}u_{x_1}^{pr}$ is the displacement of second harmonics induced by the crack-induced source at a double frequency $CISS_{2f_0}^{bre}$. k_{pr} is the wavenumber of the second harmonic at double frequency. r is the distance from the crack to the sensor. H is Hankel function. $U^n(z)$ and $W^n(z)$ represent the displacement function of the thickness coordinate for the nth Lamb wave mode. $\sigma^{Sm}(z)$ is the mode shape function for the stress field of m^{th} symmetric mode.

To evaluate the fatigue crack, an index can be accordingly defined:

$$
NI^{3D} = \frac{{}_{2f_0}u_{x_1}^{pr}}{u_{x_1}^{f_0}}. \tag{9}
$$

where $u_{x_1}^{f_0}$ is the displacement induced by incident waves at the incident frequency. Note that since the incident waves are excited by a point load, the generated waves would decay cylindrically away from the excitation source, and thus the

signals are compensated accordingly for beam spreading, so as to eliminate the influence of the decay of the incident waves, yielding

$$NI_{point\,load}^{3D} = NI^{3D} \times \frac{\sqrt{d+r}}{\sqrt{d}}. \tag{10}$$

In the above, d denotes the distance between the source of incident waves and the sensor, as shown in Figure 1.

4. VALIDATION OF THE PROPOSED MODEL USING FINITE ELEMENT METHOD

For validation of the proposed modeling approach, an aluminum plate, measuring 2 mm in thickness, 500 mm in length and 600 mm in width, was meshed and analyzed using ABAQUS®/EXPLICIT. The properties of the aluminum plate are given in Table 1.

Table 1. Properties of the aluminum Plate

Density (kg/m^3)	E (GPa)	υ	c_L (m/s)	c_T (m/s)
2660	71.8	0.33	6324	3185

The incident five-cycle Hanning-windowed sinusoidal tone bursts were applied at a pair of points which were symmetric about the medium plane of the plate in the thickness direction to excite the symmetric Lamb wave mode (S_0). To model the "breathing" crack in the plate, a seam crack was defined at the crack interface, and a contact pair interaction between the two crack surfaces was defined as well.

Under most circumstances, the amplitude of the second harmonics induced by damage in the structures is significantly smaller than that of probing waves. In order to make the second harmonics conspicuous, a pulse-inversion technique[17] was employed to extract the second harmonics, by reducing the dominance of wave modes with incident frequency. By way of illustration, results in Figure 5 demonstrate the effectiveness of this technique. After processing the acquired data with the short-time Fourier Transform (STFT) technique, respective spectrum for the original and combined signals are shown in Figure 5(b) and Figure 5 (c), from which the amplitude of the second harmonics and incident waves can be ascertained.

The correlation between the defined index and crack parameters can be accordingly obtained, as shown in Figure 6. Compared with the results obtained from the analytical method, good coincidence can be observerd. It has been demonstrated that, the severer a crack the larger the defined nonlinearity index it will be. Compared with the results obtained without considering the time-delay caused by diffracted waves, the significant influence of the diffraction on the generated nonlinearity is spotlighted, especially when the crack length reaches a certain degree. From the monotonous correlation shown in Figure 6, conclusion can be drawn that the defiend index can be used to identify the generation of the fatigue crack and to represent the severity of the crack. In real-world applications, in conjunction with the use of some previously developed techniques, such as a probability-based diagnostic imaging (PDI)[18] method, to pinpoint the location of the crack in advance, the proposed method can be used to achieve an evaluation of cracks in a quantitative manner.

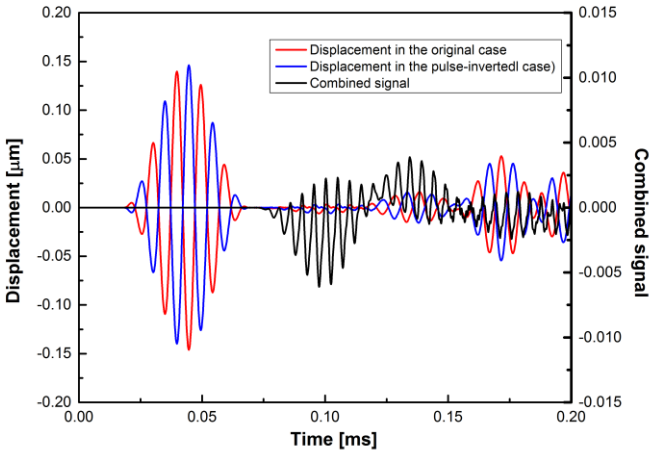

(a)

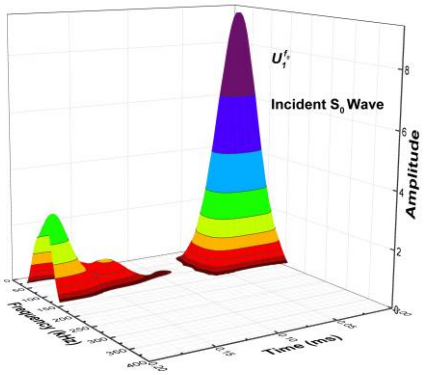

(b)

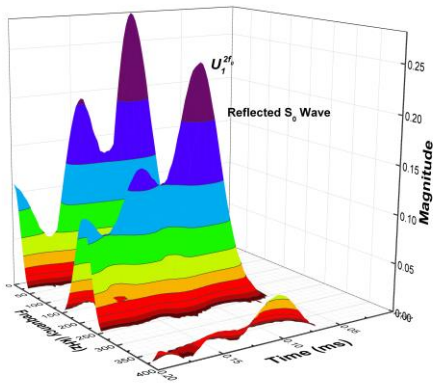

(c)

Figure 5 (a) Obtained signals (in simulation) in the original case, pule-inverted case and the combination of signals in both cases; (b) spectrum of the original signals; (c) spectrum of the combined signal

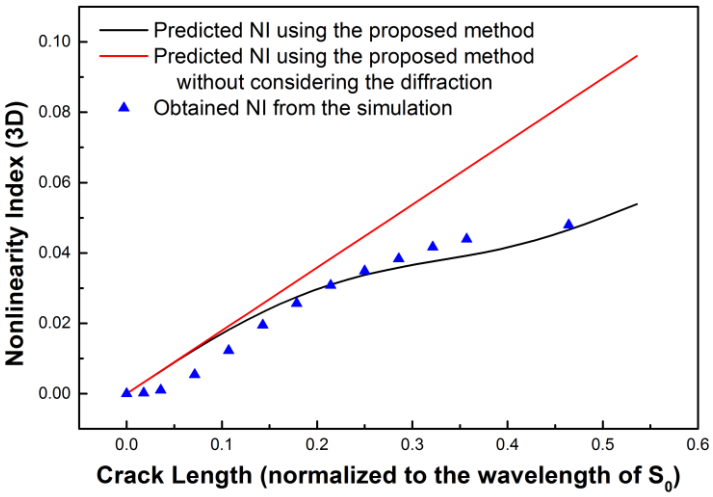

Figure 6 Nonlinearity index against the crack length (normalized to the wavelength of S_0)

5. CONCLUSIONS AND DISCUSSIONS

In this study, we develop an analytical method to interpret the generation of CAN in the 3-D scenario when probing waves traversing the "breathing" crack, whereby the evaluation of the fatigue crack can be obtained using the CAN. In this method, the "breathing" behavior of the fatigue crack is scrutinized by analyzing the motion of crack surfaces in the time domain, yielding the analytical depiction of the CISS at the crack. In conjunction with the use of an elasto-dynamic method, the accordingly generated propagating second harmonics can be analytically predicted. With the prediction, a nonlinearity index is defined to represent the severity of the fatigue crack. Validation of the proposed method is fulfilled by comparing its results with that from the finite element simulation, yielding good coincidence. The influence of the orientation of the crack on the generation of CAN needs to be investigated in the further research.

ACKNOWLEDGMENTS

This project is supported by National Natural Science Foundation of China (Key Project No. 51635008, and General Project No. 51375414). This study is also supported by the Hong Kong Research Grants Council via General Research Funds (GRF Nos. 15201416, 523313 and 15214414).

REFERENCES

[1]. Wang, K. and Z. Su. "Analytical modeling of contact acoustic nonlinearity of guided waves and its application to evaluating severity of fatigue damage". in *SPIE Smart Structures and Materials+ Nondestructive Evaluation and Health Monitoring*. 2016. International Society for Optics and Photonics.

[2]. Balageas, D.L., "Structural health monitoring R&D at the "European Research Establishments in Aeronautics"(EREA)." Aerospace science and technology, 2002. 6(3): p. 159-170.

[3]. Montalvao, D., N.M.M. Maia, and A.M.R. Ribeiro, "A review of vibration-based structural health monitoring with special emphasis on composite materials." Shock and Vibration Digest, 2006. 38(4): p. 295-324.

[4]. Moyo, P. and J. Brownjohn, "Detection of anomalous structural behaviour using wavelet analysis." Mechanical Systems and Signal Processing, 2002. 16(2-3): p. 429-445.
[5]. Su, Z. and L. Ye, [Identification of damage using Lamb waves: from fundamentals to applications]. Vol. 48. 2009: Springer Science & Business Media.
[6]. Su, Z., L. Ye, and Y. Lu, "Guided Lamb waves for identification of damage in composite structures: A review." Journal of sound and vibration, 2006. 295(3): p. 753-780.
[7]. Raghavan, A. and C.E. Cesnik, "Review of guided-wave structural health monitoring." Shock and Vibration Digest, 2007. 39(2): p. 91-116.
[8]. Rose, J.L., "A baseline and vision of ultrasonic guided wave inspection potential." Journal of pressure vessel technology, 2002. 124(3): p. 273-282.
[9]. Cantrell, J.H. and W.T. Yost, "Nonlinear ultrasonic characterization of fatigue microstructures." International Journal of Fatigue, 2001. 23, Supplement 1: p. 487-490.
[10]. Meo, M., U. Polimeno, and G. Zumpano, "Detecting Damage in Composite Material Using Nonlinear Elastic Wave Spectroscopy Methods." Applied Composite Materials, 2008. 15(3): p. 115-126.
[11]. Bermes, C., et al., "Nonlinear Lamb waves for the detection of material nonlinearity." Mechanical Systems and Signal Processing, 2008. 22(3): p. 638-646.
[12]. Klepka, A., et al., "Nonlinear acoustics for fatigue crack detection–experimental investigations of vibro-acoustic wave modulations." Structural Health Monitoring, 2012. 11(2): p. 197-211.
[13]. Solodov, I.Y., "Ultrasonics of non-linear contacts: propagation, reflection and NDE-applications." Ultrasonics, 1998. 36(1-5): p. 383-390.
[14]. Richardson, J.M., "Harmonic generation at an unbonded interface—I. Planar interface between semi-infinite elastic media." International Journal of Engineering Science, 1979. 17(1): p. 73-85.
[15]. Morvan, B., et al., "Lamb wave reflection at the free edge of a plate." The Journal of the Acoustical Society of America, 2003. 113(3): p. 1417-1425.
[16]. Achenbach, J. and Y. Xu, "Wave motion in an isotropic elastic layer generated by a time-harmonic point load of arbitrary direction." The Journal of the Acoustical Society of America, 1999. 106(1): p. 83-90.
[17]. Simpson, D.H., C.T. Chin, and P.N. Burns, "Pulse inversion Doppler: a new method for detecting nonlinear echoes from microbubble contrast agents." IEEE transactions on ultrasonics, ferroelectrics, and frequency control, 1999. 46(2): p. 372-382.
[18]. Zhou, C., Z. Su, and L. Cheng, "Probability-based diagnostic imaging using hybrid features extracted from ultrasonic Lamb wave signals." Smart Materials and Structures, 2011. 20(12): p. 125005.